Gastro Hep Advances 2025;4:100557

ORIGINAL RESEARCH—BASIC

Characterization of Pancreatic Collagen-Expressing Fibroblasts in Mouse Acute Pancreatitis

Amy Qin,[1] Kevin Shi,[1] Rachel R. Tindall,[1] Jiajing Li,[1] Binglu Cheng,[1] Jing Li,[1] Baibing Yang,[1] Qiang Yu,[1] Yinjie Zhang,[1] Bangxing Hong,[2] Balveen Kaur,[2] Mamoun Younes,[3] Qiang Shen,[4] Jennifer M. Bailey-Lundberg,[5] Yanna Cao,[1] and Tien C. Ko[1]

[1]*Department of Surgery, UTHealth at Houston, Houston, Texas;* [2]*Department of Pathology, Georgia Cancer Center, Augusta University, Augusta, Georgia;* [3]*Department of Pathology, George Washington University, Washington, District of Columbia;* [4]*Department of Interdisciplinary Oncology, Louisiana State University Health Sciences Center, New Orleans, Louisiana; and* [5]*Department of Anesthesiology, Critical Care and Pain Medicine, UTHealth at Houston, Houston, Texas*

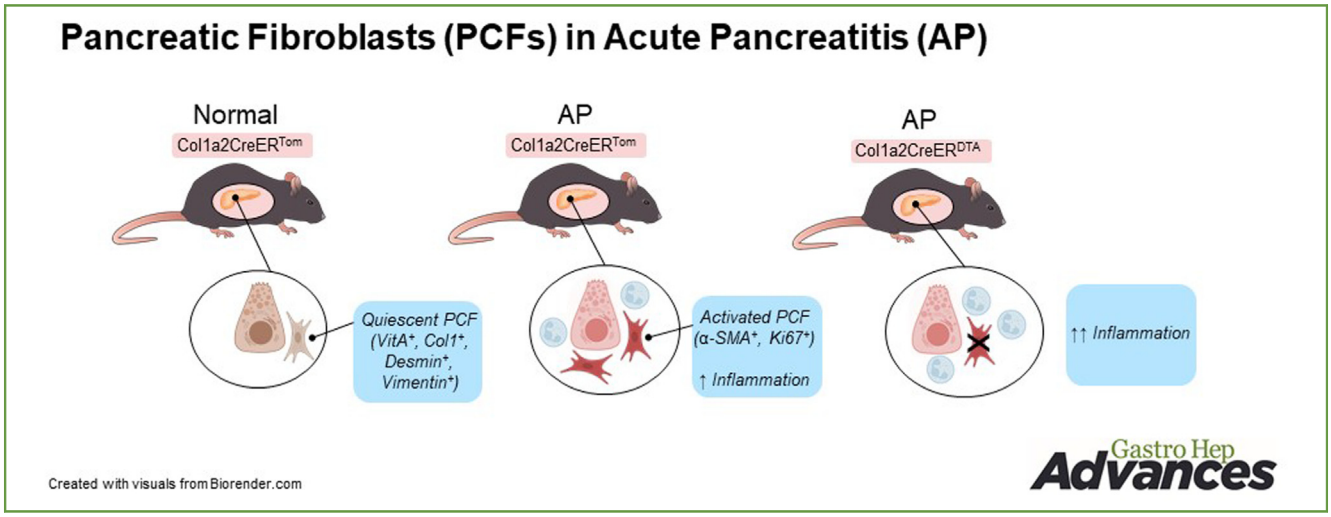

BACKGROUND AND AIMS: Pancreatic stellate cells (PSCs) are critical mediators in chronic pancreatitis with an undefined role in acute pancreatitis (AP). PSCs consist of a heterogenous group of cells and are considered interchangeable with pancreatic fibroblasts. This study explored the heterogeneous nature of PSCs by characterizing pancreatic collagen-expressing fibroblasts (PCFs) via lineage tracing in mouse normal and AP pancreas and determining the effect of PCF depletion in AP. **METHODS:** Tandem dimer Tomato (tdTom$^+$) PCFs in collagen type 1 (Col1) a2CreER$^{\text{tdTomato (Tom)}}$ mice receiving tamoxifen were characterized via fluorescence, Oil Red staining, and flow cytometry. AP was induced by cerulein, AP injury was assessed, and tdTom$^+$ PCFs were monitored. The effect of PCF depletion on AP injury was evaluated in Col1a2CreER$^{\text{diphtheria toxin A}}$ mice. **RESULTS:** Approximately 13% of pancreatic cells in Col1a2CreER$^{\text{Tom}}$ mice were labeled by tdTom (tdTom$^+$ PCFs), which surrounded acini, ducts, and blood vessels, and stained with Oil Red, collagen type I, vimentin, and desmin. tdTom$^+$ PCFs increased 2-fold during AP, correlating with AP score, amylase, and alpha-smooth muscle actin$^+$ and Ki67$^+$ staining. PCF depletion in Col1a2-CreER$^{\text{diphtheria toxin A}}$ mice receiving tamoxifen resulted in enhanced inflammation compared to control. **CONCLUSION:** PCFs may constitute a subset of PSCs and can be activated during AP. PCF depletion aggravates AP, suggesting a protective role for PCFs.

Keywords: Pancreatic Stellate Cells; Lineage Tracing; Cell Depletion; Mouse Model

Introduction

Acute pancreatitis (AP) is an inflammatory pancreatic disease characterized by severe abdominal pain and high fever. It is one of the leading gastrointestinal causes of

Abbreviations used in this paper: **α-SMA, alpha-smooth muscle actin; AP, acute pancreatitis; Col1, collagen type 1; Cox2, cyclooxygenase-2; CP, chronic pancreatitis; DTA, diphtheria toxin A; ECM, extracellular matrix; FBS, fetal bovine serum; HBSS, Hank's balanced salt solution; HSC, hepatic stellate cell; IF, immunofluorescence; Il6, interleukin 6; ip, intraperitoneal; PBS, phosphate-buffered saline; PCF, pancreatic collagen-expressing fibroblast; PDAC, pancreatic ductal adenocarcinoma; PNA, peanut agglutinin; PSC, pancreatic stellate cell; RFP, red fluorescent protein; TAM, tamoxifen; tdTom, tandem dimer Tomato; Tnfα, tumor necrosis factor alpha.**

Most current article

2772-5723
https://doi.org/10.1016/j.gastha.2024.09.012

hospitalization in the United States, accounting for approximately 300,000 emergency room visits per year.[1,2] AP arises from inciting damage to the pancreatic acinar cells, which leads to premature activation of trypsinogen into trypsin and results in autodigestion of pancreatic tissue.[3] The most common etiologies for AP are gallstones and ethanol.[1] Although most cases self-resolve, approximately 8% of AP patients will ultimately develop chronic pancreatitis (CP),[4] a disease characterized by extensive pancreatic fibrosis, chronic abdominal pain, and eventual pancreatic insufficiency.[5] CP is the most common cause of type 3c diabetes, accounting for nearly 80% of cases.[6] CP is also a significant risk factor for pancreatic ductal adenocarcinoma (PDAC), with a nearly 8-fold increased risk of PDAC within 5 years of CP diagnosis.[7] PDAC is a highly lethal cancer with a 5-year overall survival rate of less than 10%.[8] Currently, treatment for AP and CP is limited to supportive care and risk management.[1] Therefore, a better understanding of the mechanisms underlying AP and CP is critical for the development of specific therapeutics to mitigate pancreatitis and prevent disease progression to type 3c diabetes or PDAC.

In a normal pancreas, pancreatic stellate cells (PSCs) are quiescent, vitamin A lipid-storing cells that comprise 4%–7% of all pancreatic cells.[9,10] PSCs are a heterogeneous group of cells [11,12] and their origin is still a subject of speculation. PSCs express neural markers like nestin and glial fibrillary acidic protein and could thus be derived from neural crest cells.[13] They also share significant transcriptomic and proteomic similarity to hepatic stellate cells (HSCs), which have been shown to originate from mesenchymal cells.[14] One study suggests that a proportion of PSCs may originate from bone marrow,[15] whereas another report indicates that PSCs could originate from multipotent precursors in adult mouse pancreas.[16] Thus, the heterogeneity of PSCs may be partially explained by multiple originating cell populations.

PSCs have often been considered distinct from pancreatic fibroblasts. This categorization is based on the unique vitamin A droplets in the cytoplasm of PSCs and their ability to transform into a myofibroblast-like phenotype by expressing alpha-smooth muscle actin (α-SMA) during pancreatic injury.[9,10] However, PSCs and fibroblasts are also considered by some to be interchangeable.[17] This is because many of the markers typically used to identify PSCs are nonspecific, such as glial fibrillary acidic protein, which also detects neurons, and desmin, a general fibroblast marker.[12] Thus, the current understanding of the relationship between PSCs and fibroblasts varies and demands further investigation.

Studies over the past 3 decades have shown that the activation of PSCs is central to the progression of both CP and PDAC.[18] In CP, repeated pancreatic injury activates PSCs, leading to the accumulation of an extracellular matrix (ECM)-rich stroma that disrupts standard tissue structure and function.[12,19] This secretion of ECM, including type 1 collagen (Col1), in injured tissue is associated with creating a fibrotic environment, a significant component of the tumor microenvironment that promotes carcinogenesis in PDAC.[20,21] However, the role of PSCs in AP remains largely undefined, and the lack of consensus over specific population marker genes poses a significant challenge to elucidating their origin and role in AP. Exploration of PSCs in AP is warranted to better understand their role in pathologic processes.

In this study, we explored the heterogeneous nature of PSCs by employing Col1a2CreER^{Tom} mice as a model system to genetically label pancreatic collagen-expressing fibroblasts (PCFs) with tandem dimer Tomato (tdTom) and characterize PCFs in the normal pancreas and pancreas with cerulein-induced AP. We established the validity of this *in vivo* PCF model and found that PCFs isolated from normal pancreatic tissue stained positive for vitamin A droplets, a quiescent marker of PSCs, positive for collagen type I and vimentin, and partially positive for desmin. PCFs were activated and proliferated during AP, and depletion of PCFs during AP in Col1a2CreER^{DTA} mice led to enhanced AP inflammation. Thus, our results demonstrate that PCFs may comprise a subset of PSCs with a potential protective role in AP.

Materials and Methods

Reagents

Cerulein (caerulein, CAE) was purchased from Bachem Americas, Inc (Torrance, CA USA). Tamoxifen (TAM, Sigma-Aldrich, St. Louis, MO USA), corn oil (ACH Food Companies, Oakbrook Terrace, IL USA), Phadebas Amylase test tablets (Fisher Scientific, Hampton, NH USA), peanut agglutinin (PNA)-fluorescein (Vector Laboratories, Newark, CA USA), desmin (Des)-AF488, Ki67-FITC, and α-SMA-FITC (Thermo Fisher Scientific, Fremont, CA USA), CD31-AF488, Collagen type I (Col)-FITC, and Vimentin (Vim)-AF647 (Abcam, Waltham, MA USA) were purchased.

Animals

All animal experiments were performed according to the protocols approved by the Animal Welfare Committee of UTHealth at Houston. All mice were housed in a climate-controlled room with an ambient temperature of 23 °C and a 12:12-hour light-dark cycle. Animals were fed standard rodent chow and given water ad libitum. Both male and female mice (6–8 weeks old) were used. All mice were on C57BL/6 background. The respective sibling littermates were used as controls. Col1a2CreER mice[22] (B6.Cg-Tg(Col1a2-cre/ERT,-ALPP)7Cpd/J, Stock #029567, Jackson Laboratory, Bar Harbor, ME USA) were crossbred with reporter mice tdTomato (tdTom or Tom)[23](B6.Cg-Gt(ROSA)26Sortm14(CAG-tdTomato)Hze/J, Stock # 007914, Jackson Laboratory) and produced Col1a2CreER^{Tom}. Col1a2CreER mice were crossbred with diphtheria toxin A (DTA) mice[24] (B6.129P2-Gt(ROSA)26Sortm1(DTA)Lky/J, Stock # 009669, Jackson Laboratory) and produced Col1a2CreER^{DTA} mice. The resulting animals were genotyped following specific instructions from Jackson Laboratory.

AP Induction and PCF Depletion In Vivo

Col1a2CreER^{Tom} mice were administered TAM (1 mg/day, consecutive 5 days, intraperitoneal (ip)) to induce Cre recombination. The mice were euthanized 2 days after TAM injections, the mouse blood, pancreata, and other organs were harvested. For the controls, corn oil was administered to

Col1a2CreER^{Tom} mice, or TAM was administered to tdTom mice. For AP groups, cerulein was administered (50 μg/kg, 9 hourly injections, ip) 2–5 days after TAM injection. Phosphate-buffered saline (PBS) was issued with the same volume and frequency for the control groups. The mice were euthanized at 1, 24, and 48 hours after the last injection. For Col1a2CreER^{DTA} or sibling control mice (including DTA and Col1a2CreER), TAM was administered (3 mg/mouse, consecutive 2 days, ip) and was followed by administration of cerulein (50 μg/kg, 7 hourly injections, ip) 2 days after. The mice were euthanized 17 hours after the last injection, and the mouse blood and pancreata were collected. The tissue samples were fixed in 10% formalin and paraffin embedded for morphological studies, or fixed in 4% paraformaldehyde and 10% sucrose, followed by optimal cutting temperature block preparation for frozen sectioning[25] for epifluorescence or immunofluorescence (IF).

Amylase Measurement

Serum amylase levels were measured using the Phadebas Amylase test tablets as previously described.[26,27]

Morphological Examination

Paraffin-embedded tissue samples were sectioned (5 μm thick) and stained with hematoxylin and eosin. A semi-quantitative histological scoring system of AP severity was conducted by an experienced pathologist blinded to the sample identity. Histopathological changes of AP were scored based on the extent of edema, acinar necrosis, and inflammation. Edema was scored from 0 (absent) to 4 based on the degree of expansion of interlobular septae, interacinar septae, and intercellular spaces. Acinar necrosis was scored from 0 to 4 based on the number of necrotic cells detected per high-powered field. Inflammation was scored from 0 to 4 based on the number of intralobular or perivascular leukocytes per high-power field. The resulting scores were summed to create an overall AP score.[26–28]

PCF Isolation, Oil Red Staining, and Epifluorescence Illumination

PCFs were isolated by outgrowth methods from the mouse pancreas.[10,29] The pancreatic tissue samples were minced into 1–3 cubic mm pieces in wash buffer I (Hank's balanced salt solution (HBSS) without Ca^{++} and Mg^{++}, 10% fetal bovine serum (FBS), and 0.1 mg/mL soybean trypsin inhibitor), and then rinsed with wash buffer II (HBSS, 2% FBS, and 4% bovine serum albumin) by centrifuging at 400g for 5 min. The pellet was resuspended in digestive buffer (HBSS, 8% FBS, 2 mg/mL collagenase IV, and 20 μg/mL DNase I) and incubated at 30 °C for 15 minutes. The suspension was vortexed and filtered through a 100 μm pore size filter and rinsed with wash buffer II, resuspended in growth medium (DMEM, 10% FBS, and 1xpenicillin-streptomycin), and seeded on collagen-coated cell culture plates. The cells were cultured for 2–3 days and then stained with Oil Red as described.[30,31] The tdTom epifluorescence was illuminated and captured prior to Oil Red staining.

PNA Staining and Immunostaining

Frozen tissue blocks were cut to yield 5 μm sections for epifluorescence of tdTom, PNA-fluorescein staining (1:250), IF using primary antibodies of Des-AF488 (1:100), CD31-AF488 (1:100), Ki67-FITC (1:100), and α-SMA-FITC (1:250). Non-overlapping high-power field images (5-7 images/section) were acquired using a Nikon Tie microscope and quantified using Nikon Elements AR 3.2 software (Nikon Instruments, Melville, NY USA) as previously described.[31]

Flow Cytometry

Single-cell suspension from the pancreas was prepared and flow cytometry assays were performed as described[27,32,33] using antibodies of Des-AF488 (1:100), Col-FITC (1:100), and Vim-AF647 (1:100).

RNA Extraction and Quantitative Polymerase Chain Reaction

Total RNA was extracted from pancreatic tissue samples using RNeasy Plus Universal Mini Kit (Qiagen Sciences Inc, Germantown, MD, USA) and reversely transcribed to complementary (c)DNA using SuperScript IV First-Strand Synthesis kit (ThermoFisher Scientific, Waltham, MA, USA). Quantitative polymerase chain reaction was conducted as previously described[31] using TaqMan gene expression master mix and specific gene probes for mouse interleukin 6 (Il6) (Mm00446190_m1), cyclooxygenase-2 (Cox2) (Mm00478374_m1), tumor necrosis factor alpha (Tnfα) (Mm00443260_g1), and 18S (Hs99999901_s1) (ThermoFisher Scientific). Specific signals acquired were normalized to signals acquired from 18S.

Statistical Analysis

Data are expressed as mean ± standard error (SEM). Statistical significance was determined using the Student's *t*-test. *P* values <.05 were considered statistically significant. All statistics were performed using GraphPad Prism, version 9 (GraphPad Software, La Jolla, CA USA).

Results

Col1a2CreER^{Tom} mouse model is a unique tool to track collagen-expressing fibroblasts in the pancreas and other organs

To explore the heterogenous nature of PSCs in AP, we employed Col1a2CreER^{Tom} mice as a model system to genetically label PCFs. Col1a2CreER mice express a TAM-inducible Cre-ER under the control of a fibroblast-specific regulatory sequence from the proα2 (I) collagen gene.[22] Col1a2CreER mice were crossbred with a Cre reporter mouse line, tdTom, to produce Col1a2CreER^{Tom} mice, in which the fibroblast-specific regulatory sequence is incorporated in the reporter gene in fibroblasts, thus allowing tracing of Col1-expressing fibroblasts. In order to demonstrate the specificity of Col1a2-promoter-driven labeling of PCFs, we evaluated the PCFs by quantifying tdTom illumination in the Col1a2CreER^{Tom} mouse pancreas. We observed that tdTom^{+} PCFs comprised approximately 13% of total pancreatic cells in Col1a2CreER^{Tom} mice after TAM injection (Figure 1A, upper right panel). In contrast, the control corn oil-injected Col1a2CreER^{Tom} mice rarely showed tdTom^{+}

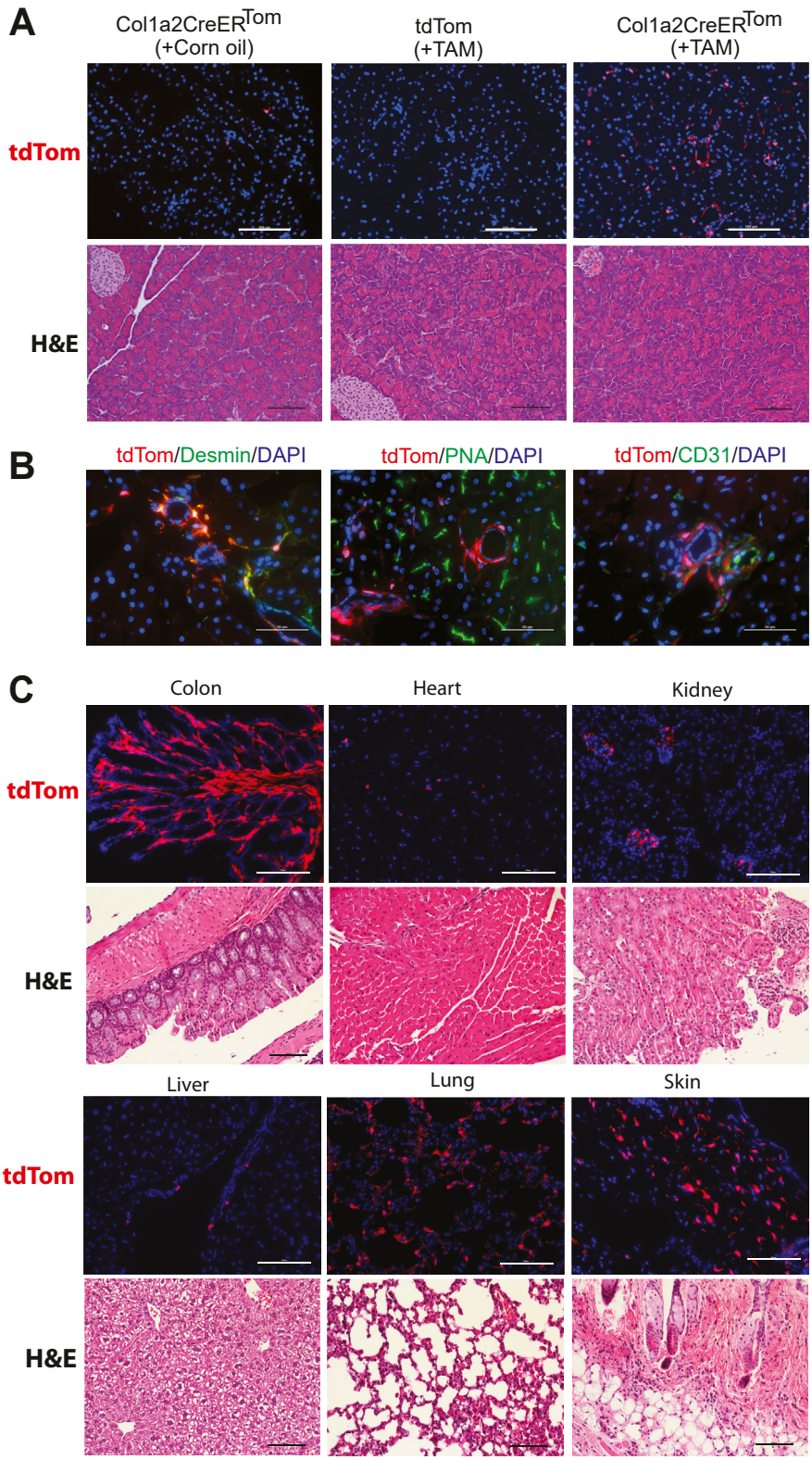

Figure 1. Characterization of Col-expressing cells in Col1a2CreER^{Tom} mouse pancreas and other organs. Mice received TAM or corn oil injections and were euthanized 2 days later. The mouse organs were harvested for analysis. (A) Representative images of tdTom epifluorescence and H&E in the pancreas from Col1a2CreER^{Tom} mice with TAM or corn oil injections, or tdTom mice with TAM injections. Scale bar = 100 μm. (B) Representative images of fluorescence in the pancreas from Col1a2CreER^{Tom} with TAM injections. Scale bar = 50 μm. (C) Representative images of tdTom epifluorescence and H&E in other organs from Col1a2CreER^{Tom} with TAM injections. Scale bar = 100 μm. n = 2-3 mice/group. H&E, hematoxylin and eosin.

cells (Figure 1A, upper left panel), and no tdTom$^+$ cells were detected in control tdTom mice with TAM injection (Figure 1A, upper middle panel). These data indicate high specificity of Col1a2CreER^{Tom} mouse model in tagging PCFs, thus validating the model system. We observed tdTom$^+$ PCFs distributed around acinar, ductal, and vascular structures and stained partially positive for desmin, negative for PNA (pancreatic acinar cell marker), and CD31 (endothelial cell marker) (Figure 1B).

We also surveyed tdTom$^+$ fibroblasts in multiple vital organs, including the colon, heart, kidney, liver, lung, and skin. The tdTom + fibroblasts were detected at levels

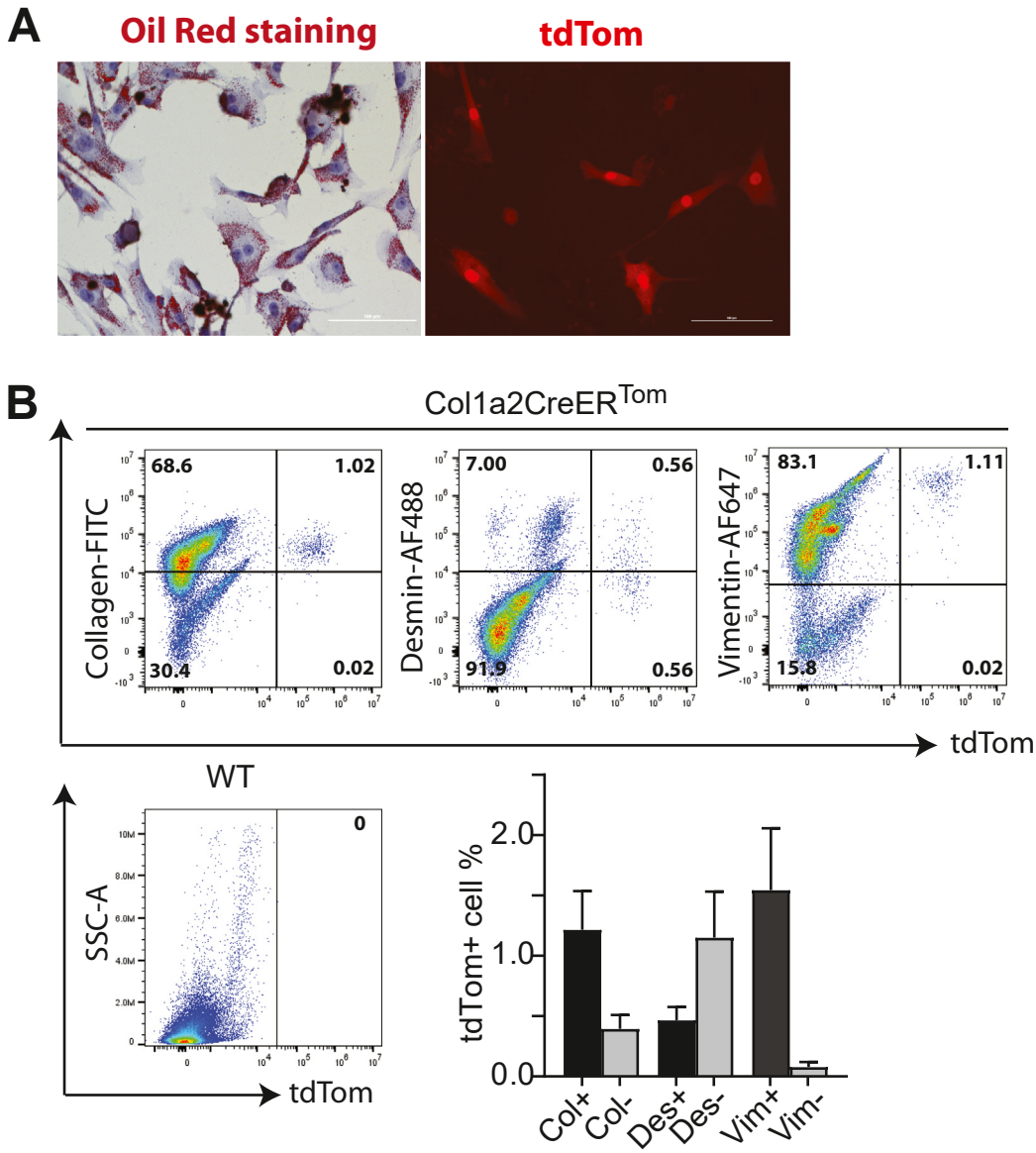

Figure 2. Characterization of PCFs *ex vivo* isolated from Col1a2CreER^{Tom} mice. Col1a2CreER^{Tom} mice received TAM injections and were euthanized 2 days later. The pancreata were harvested for cell isolation and analysis. (A) Representative images of Oil Red staining matched with tdTom epifluorescence from the same microscopic field. Scale bar = 100 μm. (B) Flow cytometry and quantification showing the proportion (%) of pancreatic cells of double positive for tdTom$^+$ and collagen$^+$, desmin$^+$, and vimentin$^+$ vs tdTom$^+$ only. Wild type as controls. n = 3-4 mice/group.

ranging from remarkably high in lung (65.39 ± 2.7%), skin (51.69 ± 0.6%), and colon (32.87 ± 5.4%) to low in kidney (5.43 ± 0.3%), heart (4.56 ± 1.9%), and liver (0.92 ± 0.4%) (Figure 1C, n = 2 mice).

Taken together, these data demonstrate specific labeling of PCFs in normal pancreas. The presence of tdTom-labeled fibroblasts in other organs is also evident, which may be valuable in tracking fibroblasts in other organs in normal physiologic states as well as in disease states.

tdTom$^+$ PCFs Constitute a Subset of PSCs

To further characterize PCFs in normal pancreas, we utilized the outgrowth method of PCFs isolated from the mouse pancreas,[10,29] and performed Oil Red staining to detect vitamin A lipid droplets,[30,31] a specific marker for quiescent PSCs. We found that nearly all outgrowth cells were positive for Oil Red staining, and tdTom$^+$ cells constituted approximately 35% of Oil Red-positive stained cells (Figure 2A). We prepared a single-cell suspension from the pancreas of Col1a2CreER^{Tom} mice and quantified the prevalence of commonly used PSC markers using flow cytometry. As shown in Figure 2B, 75% of tdTom$^+$ cells were collagen$^+$, 29% were desmin$^+$, and 95% were vimentin$^+$. These data suggest that tdTom$^+$ PCFs constitute a subset of heterogeneous PSCs in the pancreas.

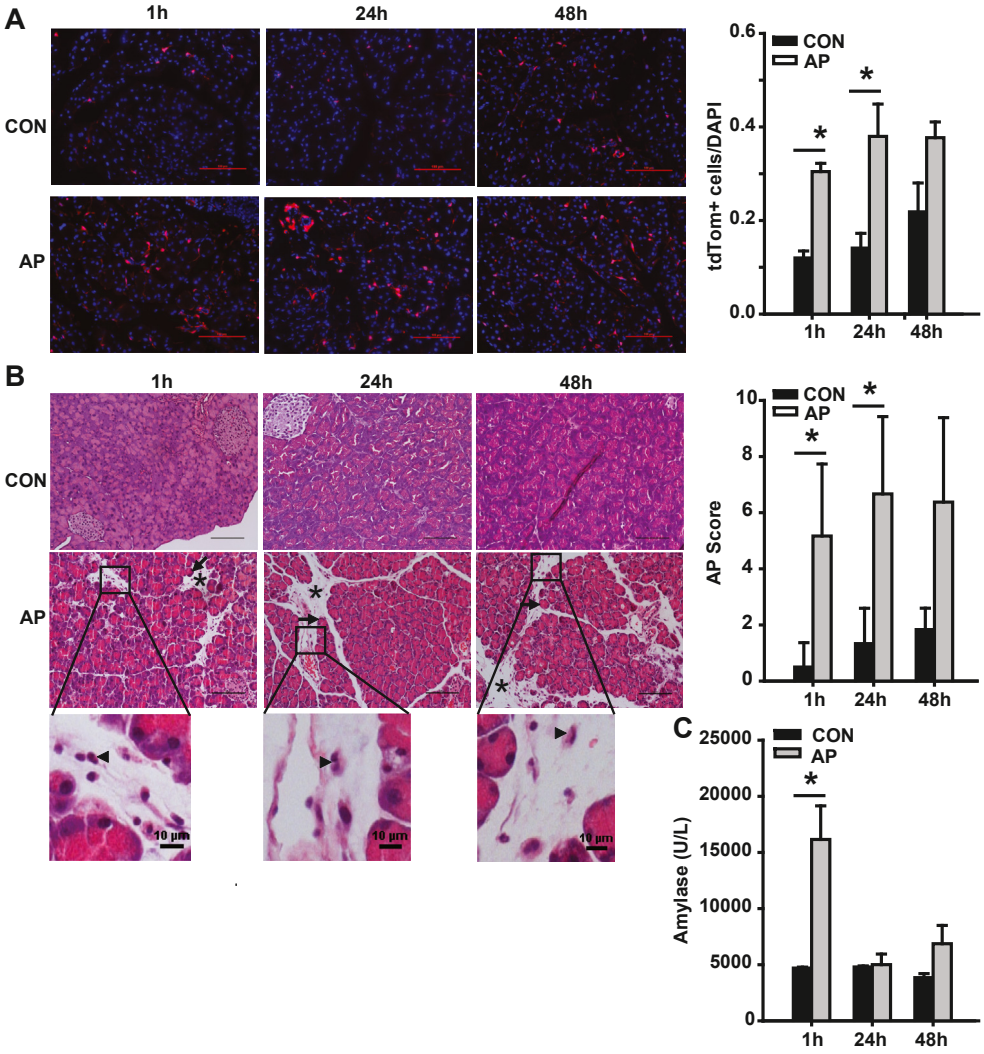

Figure 3. Increased PCFs during AP induction in Col1a2CreER^{Tom} mice. Col1a2CreER^{Tom} mice received cerulein (50 μg/kg, 9 hourly, ip) or PBS after TAM injections and were euthanized at indicated time points after the last injection. The sera and pancreata were collected. (A) tdTom epifluorescence and quantification. Scale bar = 100 μm. (B) H&E images and AP scores. Scale bar = 100 μm. (C) Amylase levels. *$P < .05$. n = 3-4/group. Asterisks indicating edema, arrows indicating necrosis, and arrowheads indicating neutrophils or polymorphonuclear leukocytes (PMNs) for inflammation. H&E, hematoxylin and eosin.

tdTom$^+$ PCFs Are Activated and Proliferate During AP Induction

In order to trace the fate of PCFs over the disease course of AP, we used cerulein to induce AP in Col1a2CreER^{Tom} mice after TAM injection. Compared to the control mice, the tdTom$^+$ PCFs were significantly increased upon AP induction at 1- and 24-hour time points ($P < .05$, Figure 3A). The increases in tdTom$^+$ PCFs during AP induction were paralleled by increased AP severity scores compared to controls ($P < .05$, Figure 3B). Serum amylase was also elevated at 1-hour time point compared to controls ($P < .05$, Figure 3C).

To investigate the activation status of tdTom$^+$ PCFs over the course of AP, we performed IF staining using α-SMA, a marker of activated, myofibroblast-like cells.[11] We observed significant increases of α-SMA$^+$ tdTom$^+$ PCFs in AP groups at 24 and 48 hours after AP induction compared to PBS control groups ($P < .05$, Figure 4A), indicating activation of PCFs during AP. Furthermore, we performed IF staining using a cell proliferation marker, Ki67, and found significant increases of Ki67$^+$tdTom$^+$ PCFs in AP groups at 24 and 48 hours after AP induction compared to PBS control groups ($P < .05$, Figure 4B). No significant differences of α-SMA and Ki67 staining were observed between control and AP groups at 1 hour after AP induction. Taken together, these data demonstrated that tdTom$^+$ PCFs were activated, attained a myofibroblast-like phenotype, and proliferated over the progression of AP.

Depletion of PCFs in Col1a2CreER^{DTA} Mice Results in Enhanced AP Inflammation

To elucidate the role of PCFs in AP, we utilized Col1a2-CreER^{DTA} mouse model to study the effects of PCF depletion on AP *in vivo*. Col1a2CreER^{DTA} mice were generated by in-house crossbreeding of Col1a2CreER with diphtherial toxin A (DTA) mice, which are genetically modified mice expressing DTA under the control of a loxP-flanked stop cassette[24]; TAM administration induces DTA expression in Col1a2CreER^{DTA} mice, leading to depletion of PCFs. This study subjected Col1a2CreER^{DTA} and control mice (including DTA and Col1a2CreER) to TAM administration followed by AP induction with cerulein injections. Administration of TAM with ip injections for 5 consecutive days at

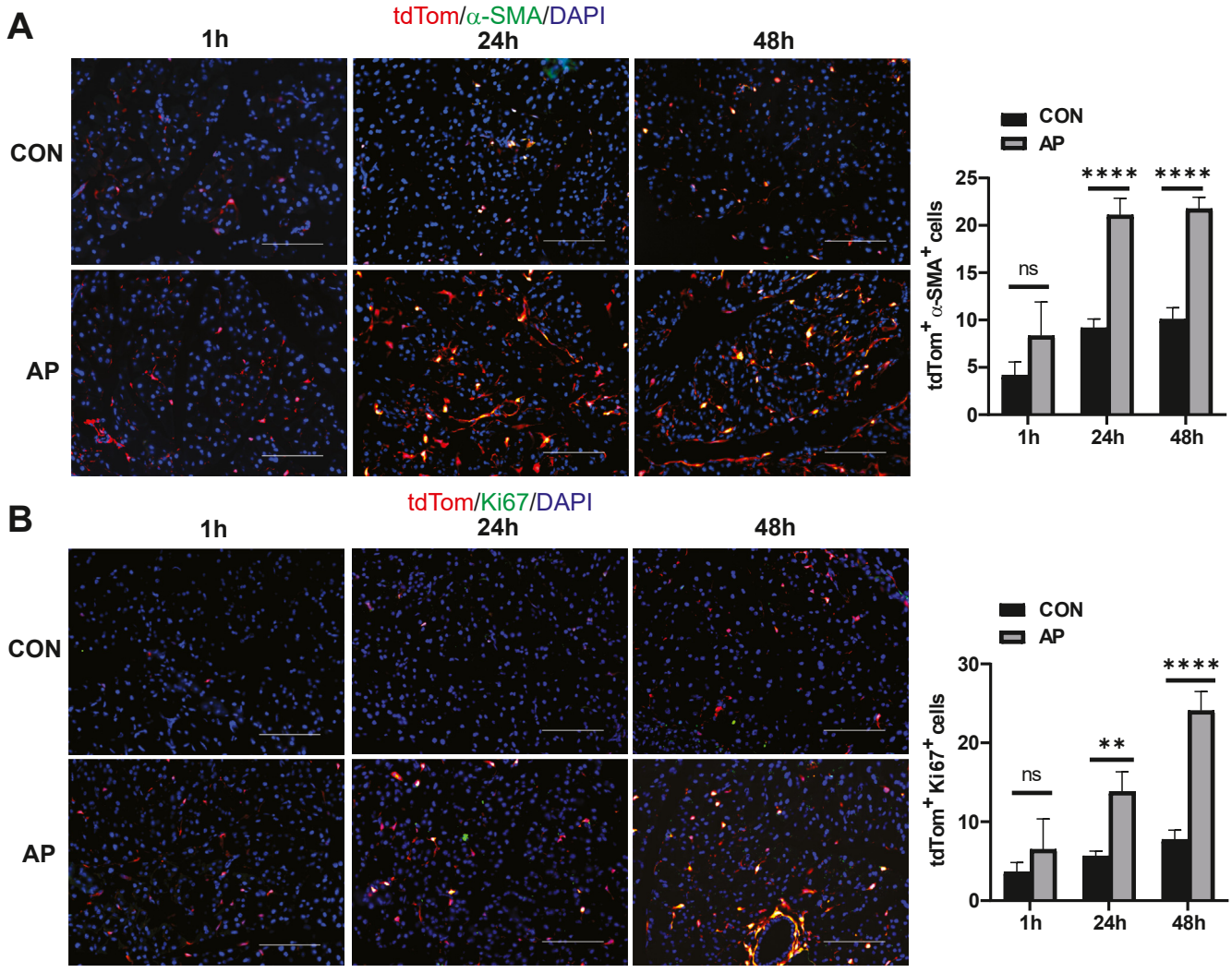

Figure 4. Activation and proliferation of PCFs in Col1a2CreER^{Tom} mice. Pancreas sections from the same set of mice described in Figure 3. (A) Representative images of IF with α-SMA staining and quantification. (B) Representative images of IF with Ki67 staining and quantification. Scale bar = 100 μm. $^{**}P < .01$, $^{****}P < .0001$. n = 6 (3 fields/mouse from 2 mice/group/time point).

1 mg/mouse has been reported effective for Cre recombination in Col1a2CreER mice[22] and was employed in our current study for the Col1a2CreER^{Tom} mice. Since the cerulein-induced AP model requires multiple ip injections within a single day, in order to reduce the potential compounding or side effects of multiple ip injections derived from TAM, we further optimized TAM administration and shortened the TAM ip injections to 2 consecutive days at 3 mg/day (with a similar total TAM dosage of 6 mg/mouse as the 5 days' regimen of 5 mg/mouse). We compared these 2 regimens and found that they yielded similar numbers of tdTom$^+$ cells in the pancreas, 9.48 ± 1.2% (5 days at 1 mg/mouse/day) vs 12.99 ± 1.4% (2 days at 3 mg/mouse/day, $P = .0847$, n = 2-3 mice/group). These results indicate that the shortened TAM administration regimen is as effective as the 5-day regimen on Cre recombination. Therefore, we applied the shortened TAM administration regimen to Col1a2CreER^{DTA} in subsequent studies.

We used different cerulein doses for the Col1a2-CreER^{Tom} and Col1a2CreER^{DTA} experimental groups because, in line with our hypothesis that PCFs exert a protective effect in AP, their depletion was anticipated to exacerbate AP. As shown in Figure 3B, 9 hourly cerulein injections induced AP injury approaching the maximum effects of the cerulein at 24 hours after cerulein administration. In order to determine differences in AP severity between Col1a2CreER^{DTA} and control mice, we chose a lower cerulein dose with 7 hourly injections for a submaximal AP injury in the control mice. We euthanized Col1a2-CreER^{DTA} and control mice at a single time point at 17 hours after completion of cerulein administration. According to the time course of cerulein-induced AP that we established in Col1a2CreER^{Tom} mice, which showed elevated serum amylase levels and AP scores at 1 hour and elevated AP scores until 48 hours, at the 17 hour time point, the mouse pancreatic AP injury may still fall within the acute phase. As

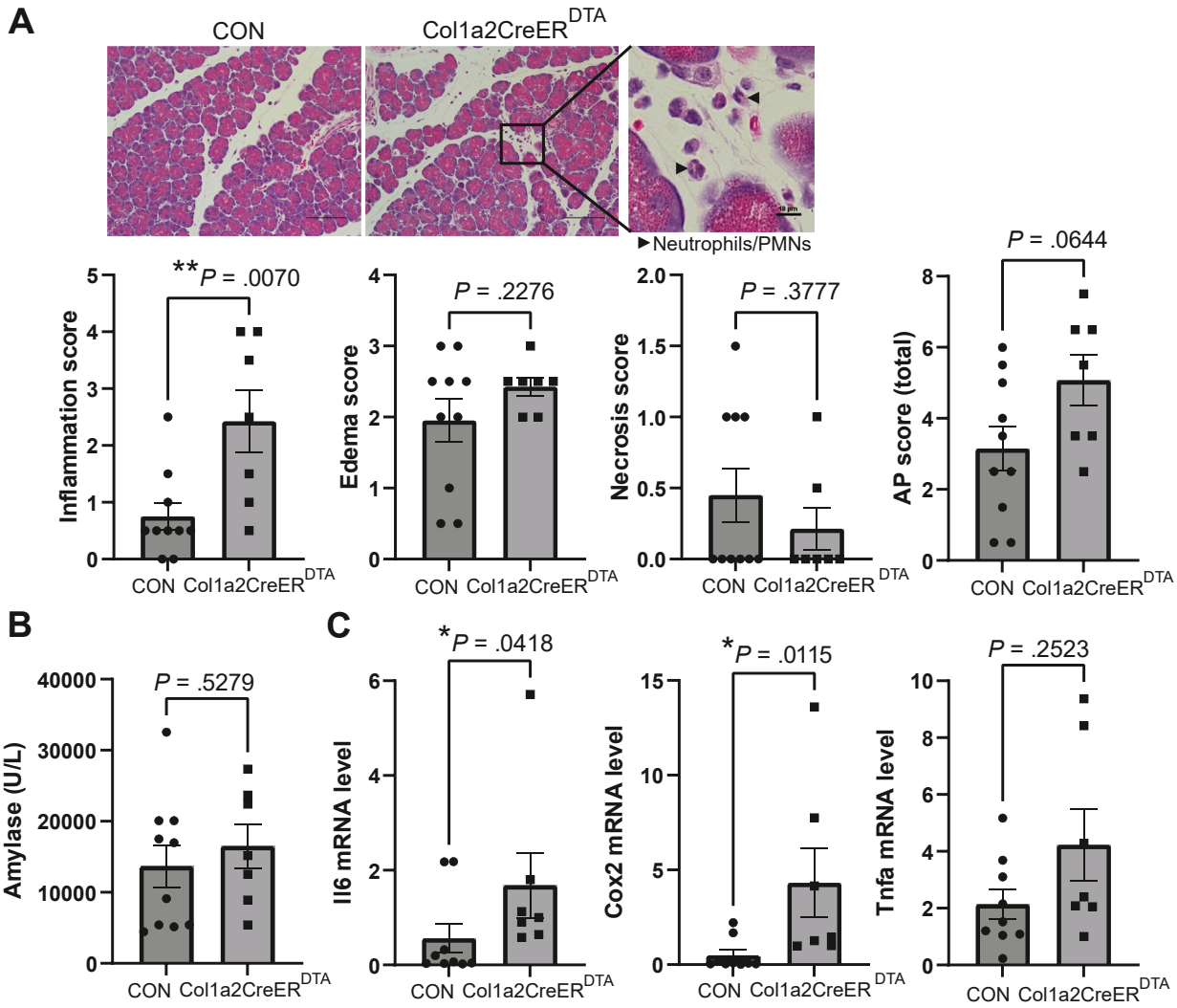

Figure 5. Effects of PCF depletion on AP injury in Col1a2CreER^{DTA} mice. Col1a2CreER^{DTA} or control mice (sibling littermates including DTA and Col1a2CreER mice) received cerulein (50 μg/kg, 7 hourly, ip) 2 days after TAM injection (3 mg/mouse, consecutive 2 days, ip) and were euthanized 17 hours after the last cerulein injection. The serum and pancreata were collected. (A) H&E images, inflammation, edema, necrosis, and overall AP scores. Scale bar = 100 μm. (B) Serum amylase levels. (C) Il6, Cox2, and Tnfα mRNA levels measured by qPCR. Data are presented as mean ± SEM *$P < .05$, **$P < .01$. n = 7-10 mice/group. H&E, hematoxylin and eosin; qPCR, quantitative polymerase chain reaction.

shown in Figure 5A, compared to the control mouse pancreas, Col1a2CreER^{DTA} mouse pancreas exhibited increased inflammation score ($P < .05$) and marginal increased total AP score ($P = .064$). No significant differences of edema and necrosis scores (Figure 5A) or serum amylase levels (Figure 5B) were observed between control and Col1a2CreER^{DTA} mice.

As reported, it was challenging to evaluate recombination efficiency in Col1a2CreER mice in prior studies. Kimura et al. investigated the cell fates of collagen-expressing cells in liver regeneration and found that the recombination efficiency for TAM-inducible Col1a2CreER/red fluorescent protein (RFP) mice was approximately 26% based on RFP$^+$ cell counts per α-SMA$^+$ cells.[34] Another study by Chan et al. found that estimation of recombination efficiency using RFP expression tended to underestimate recombination efficiency.[35] Li et al. investigated the role of Smad7 in CP by utilizing a mouse model with Col1a2CreER with Smad7 knockout. They observed around 85% Smad7 gene knockout from isolated pancreatic fibroblasts but could not determine recombination frequency of Col1a2CreER allele *in vivo*.[36] In the current study, we found that tdTom$^+$ cells comprised 35% of Oil Red$^+$ cells, as shown in Figure 2A, which may serve as an estimate of recombination efficiency in Col1a2CreER^{Tom} mice. These varying results indicate that recombination efficiency is likely low in the pancreas and liver. However, we observed remarkably high levels of tdTom$^+$ cells in lung, skin, and colon tissues. Whether the organ-dependent differences of tdTom$^+$ cells are due to the differences in recombination efficiency or to actual differences in the number of fibroblasts warrants further validation. Another challenge to evaluating recombination

efficiency is that there are no available specific markers for fibroblasts. In this study, we used desmin, a commonly used fibroblast marker, and performed IF to directly estimate depletion efficiency of the PCFs in the same sets of Col1a2CreER^{DTA} and the control DTA mice under AP induction as in Figure 5. We observed that desmin^{+} signaling in Col1a2CreER^{DTA} mice was around 85% of the desmin^{+} signal detected in the control mice, estimating around 15% depletion of the PCFs in the Col1a2CreER^{DTA} mice.

Furthermore, we assessed Il6, Cox2, and Tnfα, which are commonly used inflammatory markers in AP. We found that Il6 and Cox2 mRNA levels were significantly higher in Col1a2CreER^{DTA} mice compared to that in control mice ($P < .05$), while no significant difference was observed in Tnfα mRNA levels (Figure 5C). These results largely corroborate the increased AP inflammation scores in Col1a2CreER^{DTA} mice with depletion of PCFs. These results suggest a potential protective, anti-inflammatory role of PCFs in AP.

Discussion

Studying PSCs is particularly challenging due to the heterogeneous nature of this cell population and lack of a universally accepted cell marker[11] or specific Cre mouse line.[37] Previously, Col1a2CreER transgenic mice have been generated in which the CreERT gene was specifically expressed in osteoblasts and odontoblasts in bone.[38] The Col1a2CreER mouse model has been used to conditionally knock out Smad7 gene in PSCs to study its fibrotic role in CP.[36] Col1a2CreER and Col1a2CreER/DTA mice have also been used to evaluate the role of collagen-expressing cells in liver regeneration and showed distinct HSC clusters, where collagen-expressing cells within the HSCs promoted liver regeneration.[34] In this study, we employed the Col1a2-CreER^{Tom} mouse model to conduct lineage tracing of PCFs in normal and AP pancreas. We showed that the Col1a2-CreER^{Tom} mouse model is capable of specifically labeling PCFs in normal and AP pancreas. Using this tool, we found that tdTom^{+} PCFs comprise 13% of total cells in normal pancreas tissue sections. We also found that PCFs constitute a fraction (35%) of Oil Red-positive cells isolated from normal pancreas, suggesting PCFs are a subset of quiescent PSCs. PCFs have varied expressions of collagen, desmin, and vimentin, which have previously been identified as markers of PSCs. Increased expression of α-SMA in AP indicates that PCFs can be transformed into an activated myofibroblast-like phenotype. Under AP induction tdTom^{+} cells not only increased in number but also became enlarged as they were activated. It has been reported that activation of PCFs results from exposure to autocrine factors as well as paracrine factors from neighboring ductal cells, acinar cells, endothelial cells, and leukocytes.[39] The proliferated tdTom^{+} cells seemed to localize predominantly around the ducts; whether this pattern serves a functional role or highlights differences in PCF responses to cerulein around ducts vs around acini warrants further studies. Our group has recently applied spatial transcriptomics to mouse AP tissue sections and identified distinct tissue clusters with differentially expressed genes,[40] which could be useful for future studies to functionally characterize periductal vs periacinar PCFs and their interactions with neighboring cells. These data show that PCFs may form a subset of PSCs rather than a distinct cellular category and that the Col1a2CreER^{Tom} mouse model is a promising tool and platform for studying PCFs in normal states.

In addition to characterizing PCFs in normal pancreas, we also monitored PCFs in the pancreas with AP in order to elucidate their role in the disease. We found that PCFs increased as AP severity increased and were activated and proliferated during the disease course. Furthermore, we employed the Col1a2CreER^{DTA} mouse model to explore the function of PCFs. We showed that the depletion of PCFs resulted in enhanced AP inflammation, suggesting that PCFs may play a protective role in AP. This is consistent with current hypotheses that PCFs may participate in repairing the pancreas after an acute inflammatory episode by providing an ECM scaffold for the restoration of acinar cells after injury.[18] These findings should prompt further investigation into the mechanistic role of PCFs in AP, which may elucidate potential therapeutic interventions for AP.

PSCs are reported to be heterogeneous. For instance, myofibroblastic PSCs are shown with elevated α-SMA and produce collagen, while inflammatory PSCs express inflammatory markers. The 2 subtypes are spatially separated, phenotypically reversible, but work synergistically to create a microenvironment conducive to cancer development.[41] Other identified PSC subtypes include CD10^{+} PSCs that promote cancer cell invasion,[42] B-cell lymphoma 2-associated athanogene 3^{+} or fibroblast activation protein^{+} PSCs that promote cancer cell migration and fibrosis,[43,44] and certain PSC populations that are tumor suppressor subtypes, such as those expressing Cd271 or Meflin.[45,46] Characterization of various PSC subsets and their roles in pancreatic cancer development may provide valuable insights into developing targeted therapies for pancreatic cancer. However, the involvement of different subtypes of PSCs in pancreatitis has been under-investigated. Future single-cell multi-omics studies into these PSC populations will shed light on the identity and function of such cells in the context of pancreatitis.

This study has several aspects of novelty. The detection of vitamin A droplets in tdTom^{+} PCFs indicates that PCFs may constitute a significant subtype of PSCs, contributing to the heterogeneous components of PSCs. The activation of PCFs during AP induction provides further evidence that PCFs may attain a myofibroblast-like phenotype as seen in activated PSCs. Our findings suggest a novel relationship between PCFs and PSCs, different from current theories suggesting they are completely distinct or interchangeable populations. Furthermore, PCFs may play an essential protective role in AP based on our observation that PCF depletion enhances AP inflammation.

This study also has limitations. Firstly, the lineage tracing model using Col1a2CreER^{Tom} showed that tdTom^{+}

PCFs comprised approximately 13% of total pancreatic cells on pancreas tissue sections; however, much lower numbers of $tdTom^+$ PCFs were obtained when pancreatic cells were isolated from the pancreas for *in vitro* assays. Thus, the *in vitro* assays may underestimate the numbers of PCFs due to loss during the *in vitro* isolation process. Additionally, this study focuses on lineage tracing of PCFs only in the AP state and does not capture the later complexities of the tissue disruption that lead to CP and PDAC. Future application of this lineage tracing model of PCFs can be extended to the studies in CP and PDAC to investigate the longitudinal role of PCFs in the spectrum of pancreatic disease. There are several more severe AP models than the cerulein-induced AP model, such as L-arginine,[47,48] lipopolysaccharide,[49] or pancreatic duct ligation[47,48] induced AP models. The cerulein-induced AP model has been widely used in the field, and we have utilized this model in our previous studies.[26,27] We therefore chose this model as the first step in exploring the heterogeneity of pancreatic fibroblasts and their potential role in AP. In future studies, we will employ additional AP models, including AP models with more severe lesions, in order to increase the robustness and further this line of research investigating the role of pancreatic fibroblasts in AP. In addition, the PCF depletion experiment in $Col1a2CreER^{DTA}$ mice on AP injury was conducted at a single time point. Future studies with multiple time points covering AP progression from acute onset to recovery are desired to further define the role of PCFs in AP.

Conclusion

In conclusion, our present study indicates that the $Col1a2CreER^{Tom}$ mouse model is a specific and effective tool to study PCFs in normal homeostasis and in disease states. Based on representative markers, our data suggest that PCFs constitute a subset of PSCs. These PCFs can be activated and proliferate during AP and may play a protective role in AP. This study provides useful models to further study the underlying mechanisms and identify potential therapeutic targets for AP.

References

1. Mederos MA, Reber HA, Girgis MD. Acute pancreatitis: a review. JAMA 2021;325(4):382–390.
2. Boxhoorn L, Voermans RP, Bouwense SA, et al. Acute pancreatitis. Lancet 2020;396(10252):726–734.
3. Bhatia M, Wong FL, Cao Y, et al. Pathophysiology of acute pancreatitis. Pancreatology 2005;5(2-3):132–144.
4. Ahmed Ali U, Issa Y, Hagenaars JC, et al. Risk of recurrent pancreatitis and progression to chronic pancreatitis after a first episode of acute pancreatitis. Clin Gastroenterol Hepatol 2016;14(5):738–746.
5. Beyer G, Habtezion A, Werner J, et al. Chronic pancreatitis. Lancet 2020;396(10249):499–512.
6. Ewald N, Kaufmann C, Raspe A, et al. Prevalence of diabetes mellitus secondary to pancreatic diseases (type 3c). Diabetes Metab Res Rev 2012;28(4):338–342.
7. Kirkegård J, Mortensen FV, Cronin-Fenton D. Chronic pancreatitis and pancreatic cancer risk: a systematic review and meta-analysis. Am J Gastroenterol 2017;112(9):1366–1372.
8. Orth M, Metzger P, Gerum S, et al. Pancreatic ductal adenocarcinoma: biological hallmarks, current status, and future perspectives of combined modality treatment approaches. Radiat Oncol 2019;14(1):141.
9. Apte MV, Haber PS, Applegate TL, et al. Periacinar stellate shaped cells in rat pancreas: identification, isolation, and culture. Gut 1998;43(1):128–133.
10. Bachem MG, Schneider E, Gross H, et al. Identification, culture, and characterization of pancreatic stellate cells in rats and humans. Gastroenterology 1998;115(2):421–432.
11. Erkan M, Adler G, Apte MV, et al. StellaTUM: current consensus and discussion on pancreatic stellate cell research. Gut 2012;61(2):172–178.
12. Garcia PE, Scales MK, Allen BL, et al. Pancreatic fibroblast heterogeneity: from development to cancer. Cells 2020;9(11):2464.
13. Lardon J, Rooman I, Bouwens L. Nestin expression in pancreatic stellate cells and angiogenic endothelial cells. Histochem Cell Biol 2002;117(6):535–540.
14. Asahina K, Zhou B, Pu WT, et al. Septum transversum-derived mesothelium gives rise to hepatic stellate cells and perivascular mesenchymal cells in developing mouse liver. Hepatology 2011;53(3):983–995.
15. Scarlett CJ, Colvin EK, Pinese M, et al. Recruitment and activation of pancreatic stellate cells from the bone marrow in pancreatic cancer: a model of tumor-host interaction. PLoS One 2011;6(10):e26088.
16. Seaberg RM, Smukler SR, Kieffer TJ, et al. Clonal identification of multipotent precursors from adult mouse pancreas that generate neural and pancreatic lineages. Nat Biotechnol 2004;22(9):1115–1124.
17. Whittle MC, Hingorani SR. Fibroblasts in pancreatic ductal adenocarcinoma: biological mechanisms and therapeutic targets. Gastroenterology 2019;156(7):2085–2096.
18. Apte M, Pirola RC, Wilson JS. Pancreatic stellate cell: physiologic role, role in fibrosis and cancer. Curr Opin Gastroenterol 2015;31(5):416–423.
19. Apte MV, Wilson JS. Mechanisms of pancreatic fibrosis. Dig Dis 2004;22(3):273–279.
20. Chen Y, Kim J, Yang S, et al. Type I collagen deletion in αSMA(+) myofibroblasts augments immune suppression and accelerates progression of pancreatic cancer. Cancer Cell 2021;39(4):548–565.e6.
21. Jin G, Hong W, Guo Y, et al. Molecular mechanism of pancreatic stellate cells activation in chronic pancreatitis and pancreatic cancer. J Cancer 2020;11(6):1505–1515.
22. Zheng B, Zhang Z, Black CM, et al. Ligand-dependent genetic recombination in fibroblasts : a potentially powerful technique for investigating gene function in fibrosis. Am J Pathol 2002;160(5):1609–1617.
23. Madisen L, Zwingman TA, Sunkin SM, et al. A robust and high-throughput Cre reporting and characterization system for the whole mouse brain. Nat Neurosci 2010;13(1):133–140.
24. Voehringer D, Liang HE, Locksley RM. Homeostasis and effector function of lymphopenia-induced "memory-like"

T cells in constitutively T cell-depleted mice. J Immunol 2008;180(7):4742–4753.
25. Kusser KL, Randall TD. Simultaneous detection of EGFP and cell surface markers by fluorescence microscopy in lymphoid tissues. J Histochem Cytochem 2003;51(1):5–14.
26. Cao Y, Yang W, Tyler MA, et al. Noggin attenuates cerulein-induced acute pancreatitis and impaired autophagy. Pancreas 2013;42(2):301–307.
27. Yang B, Davis JM, Gomez TH, et al. Characteristic pancreatic and splenic immune cell infiltration patterns in mouse acute pancreatitis. Cell Biosci 2021;11(1):28.
28. Schmidt J, Lewandrowski K, Fernandez-del Castillo C, et al. Histopathologic correlates of serum amylase activity in acute experimental pancreatitis. Dig Dis Sci 1992;37(9):1426–1433.
29. Kruse ML, Hildebrand PB, Timke C, et al. Isolation, long-term culture, and characterization of rat pancreatic fibroblastoid/stellate cells. Pancreas 2001;23(1):49–54.
30. Kim N, Yoo W, Lee J, et al. Formation of vitamin A lipid droplets in pancreatic stellate cells requires albumin. Gut 2009;58(10):1382–1390.
31. Gao X, Cao Y, Yang W, et al. BMP2 inhibits TGF-β-induced pancreatic stellate cell activation and extracellular matrix formation. Am J Physiol Gastrointest Liver Physiol 2013;304(9):G804–G813.
32. Xue J, Sharma V, Hsieh MH, et al. Alternatively activated macrophages promote pancreatic fibrosis in chronic pancreatitis. Nat Commun 2015;6:7158.
33. Zhao Q, Wei Y, Pandol SJ, et al. STING signaling promotes inflammation in experimental acute pancreatitis. Gastroenterology 2018;154(6):1822–1835.e2.
34. Kimura Y, Koyama Y, Taura K, et al. Characterization and role of collagen gene expressing hepatic cells following partial hepatectomy in mice. Hepatology 2023;77(2):443–455.
35. Chan LK, Tsesmelis M, Gerstenlauer M, et al. Functional IKK/NF-κB signaling in pancreatic stellate cells is essential to prevent autoimmune pancreatitis. Commun Biol 2022;5(1):509.
36. Li X, Nania S, Kleiter I, et al. Targeting of Smad7 in mesenchymal cells does not exacerbate fibrosis during experimental chronic pancreatitis. Pancreas 2021;50(10):1427–1434.
37. Mederacke I, Hsu CC, Troeger JS, et al. Fate tracing reveals hepatic stellate cells as dominant contributors to liver fibrosis independent of its aetiology. Nat Commun 2013;4:2823.
38. Kim JE, Nakashima K, de Crombrugghe B. Transgenic mice expressing a ligand-inducible cre recombinase in osteoblasts and odontoblasts: a new tool to examine physiology and disease of postnatal bone and tooth. Am J Pathol 2004;165(6):1875–1882.
39. Omary MB, Lugea A, Lowe AW, et al. The pancreatic stellate cell: a star on the rise in pancreatic diseases. J Clin Invest 2007;117(1):50–59.
40. Tindall RR, Yang Y, Hernandez I, et al. Aging- and alcohol-associated spatial transcriptomic signature in mouse acute pancreatitis reveals heterogeneity of inflammation and potential pathogenic factors. J Mol Med (Berl) 2024;102(8):1051–1061.
41. Öhlund D, Handly-Santana A, Biffi G, et al. Distinct populations of inflammatory fibroblasts and myofibroblasts in pancreatic cancer. J Exp Med 2017;214(3):579–596.
42. Ikenaga N, Ohuchida K, Mizumoto K, et al. CD10+ pancreatic stellate cells enhance the progression of pancreatic cancer. Gastroenterology 2010;139(3):1041–1051, 1051.e1-8.
43. Yuan Y, Jiang JY, Wang JM, et al. BAG3-positive pancreatic stellate cells promote migration and invasion of pancreatic ductal adenocarcinoma. J Cell Mol Med 2019;23(8):5006–5016.
44. Feig C, Jones JO, Kraman M, et al. Targeting CXCL12 from FAP-expressing carcinoma-associated fibroblasts synergizes with anti-PD-L1 immunotherapy in pancreatic cancer. Proc Natl Acad Sci U S A 2013;110(50):20212–20217.
45. Mizutani Y, Kobayashi H, Iida T, et al. Meflin-positive cancer-associated fibroblasts Inhibit pancreatic carcinogenesis. Cancer Res 2019;79(20):5367–5381.
46. Nielsen MFB, Mortensen MB, Detlefsen S. Typing of pancreatic cancer-associated fibroblasts identifies different subpopulations. World J Gastroenterol 2018;24(41):4663–4678.
47. Hyun JJ, Lee HS. Experimental models of pancreatitis. Clin Endosc 2014;47(3):212–216.
48. Lerch MM, Gorelick FS. Models of acute and chronic pancreatitis. Gastroenterology 2013;144(6):1180–1193.
49. Vaccaro MI, Calvo EL, Suburo AM, et al. Lipopolysaccharide directly affects pancreatic acinar cells: implications on acute pancreatitis pathophysiology. Dig Dis Sci 2000;45(5):915–926.

Received January 3, 2024. Accepted September 16, 2024.

Correspondence:
Address correspondence to: Yanna Cao, MD, Department of Surgery, UTHealth at Houston, 6431 Fannin St., MSB4.608, Houston, Texas 77030. e-mail: Yanna.Cao@uth.tmc.edu. Tien C. Ko, MD, Department of Surgery, UTHealth at Houston, 5656 Kelly, 30S62008, Houston, Texas 77026. e-mail: Tien.C.Ko@uth.tmc.edu.

Acknowledgments:
The authors thank the HistoCore Lab at UTHealth Houston for tissue process and H&E staining.

Authors' Contributions:
All authors contributed to the conception and design of the study. Generation, collection, assembly, analysis and/or interpretation of data were performed by Amy Qin, Kevin Shi, Rachel R. Tindall, Jiajing Li, Binglu Cheng, Jing Li, Baibing Yang, Qiang Yu, Yinjie Zhang, Bangxing Hong, Mamoun Younes, Jennifer M. Bailey-Lundberg, and Yanna Cao. The drafting and revisions of the manuscript were written by Amy Qin, Kevin Shi, Rachel R. Tindall, and Yanna Cao. All authors commented on the drafting and revisions of the manuscript. All authors read and approved the final version of the manuscript.

Conflicts of Interest:
The authors disclose no conflicts.

Funding:
This work was partially supported by the NIH 1R21 AA027014-01A1 and Jack H Mayfield M.D. Distinguished Professorship in Surgery (Tien C. Ko), Dean's fund for Summer Research Program at UTHealth MMS (Amy Qin, Kevin Shi, Rachel R. Tindall). The above sponsors had no involvement in the study design, collection, analysis, or interpretation of data.

Ethical Statement:
All animal experiments were performed according to the protocols approved by the Animal Welfare Committee of UTHealth at Houston.

Data Transparency Statement:
All data, analytic methods, and study materials will be available to other researchers upon reasonable request.

Reporting Guidelines:
ARRIVE/Care and Use of Laboratory Animals.